Rotatable illusion media for manipulating terahertz electromagnetic waves

XiaoFei Zang,[1] Zhou Li,[1] Cheng Shi,[1] Lin Chen,[1] Bin Cai,[1] YiMing Zhu,[1,*] Li Li,[2] and XiaoBin Wang[2]

[1]*Engineering Research Center of Optical Instrument and System, Ministry of Education and Shanghai Key Lab of Modern Optical System, University of Shanghai for Science and Technology, No.516 JunGong Road, Shanghai 200093, China*

[2]*Science and Technology on Electromagnetic Scattering Laboratory, Shanghai, China*

[*]*ymzhu@usst.edu.cn*

Abstract: Based on composite optical transformation, we propose a rotatable illusion media with positive permittivity and permeability to manipulate terahertz waves, and a new way to realize singular parameter-independent cloaks when the incident wave with a certain width propagates from specific incident directions. The fundamental mechanism of this kind of cloak is that the illusion media can be able to avoid the incident wave interacting with the objects. Comparing with traditional transformation-coordinate-based cloaks such as cylindrical-shaped cloaks, our cloaks are independent of singular material parameters. Furthermore, this type of rotatable illusion media can be applied to design tunable miniaturized high-directivity antenna (a small antenna array covered with the rotatable illusion media appears like a large one and meanwhile, the radiation directions of the small antenna array is tunable via this rotatable illusion media). Full wave simulations are performed to confirm these points.

OCIS codes: (160.3918) Metamaterials; (230.0230) Optical devices; (260.2710) Inhomogeneous optical media.

References and links

1. J. B. Pendry, D. Schurig, and D. R. Smith, "Controlling electromagnetic fields," Science **312**(5781), 1780–1782 (2006).
2. U. Leonhardt, "Optical conformal mapping," Science **312**(5781), 1777–1780 (2006).
3. W. Cai, U. K. Chettiar, A. V. Kildishev, and V. M. Shalaev, "Optical cloaking with metamaterial," Nat. Photonics **1**(4), 224–227 (2007).
4. H. S. Chen, B.-I. Wu, B. L. Zhang, and J. A. Kong, "Electromagnetic wave interactions with a metamaterial cloak," Phys. Rev. Lett. **99**(6), 063903 (2007).
5. B. L. Zhang, H. Chen, B. I. Wu, and J. A. Kong, "Extraordinary Surface Voltage Effect in the Invisibility Cloak with an Active Device Inside," Phys. Rev. Lett. **100**(6), 063904 (2008).
6. H. Y. Chen, C. T. Chan, and P. Sheng, "Transformation optics and metamaterials," Nat. Mater. **9**(5), 387–396 (2010).
7. D. Schurig, J. B. Pendry, and D. R. Smith, "Calculation of material properties and ray tracing in transformation media," Opt. Express **14**(21), 9794–9804 (2006).
8. F. Zolla, S. Guenneau, A. Nicolet, and J. B. Pendry, "Electromagnetic analysis of cylindrical invisibility cloaks and the mirage effect," Opt. Lett. **32**(9), 1069–1071 (2007).
9. W. X. Jiang, T. J. Cui, X. M. Yan, Q. Cheng, R. P. Liu, and D. R. Smith, "Invisibility cloak without singularity," Appl. Phys. Lett. **93**(19), 194102 (2008).
10. C. W. Qiu, L. Hu, B. L. Zhang, B. I. Wu, S. G. Johnson, and J. D. Joannopoulos, "Spherical cloaking using nonlinear transformations for improved segmentation into concentric isotropic coatings," Opt. Express **17**(16), 13467–13478 (2009).
11. W. R. Zhu, C. L. Ding, and X. P. Zhao, "Numerical method for designing acoustic cloak with homogeneous metamaterials," Appl. Phys. Lett. **97**(13), 131902 (2010).
12. W. R. Zhu, I. Shadrivov, D. Powell, and Y. Kivshar, "Hiding in the corner," Opt. Express **19**(21), 20827–20832 (2011).
13. H. Y. Chen and C. T. Chan, "Transformation media that rotate electromagnetic fields," Appl. Phys. Lett. **90**(24), 241105 (2007).

#195925 - $15.00 USD Received 20 Aug 2013; revised 20 Sep 2013; accepted 20 Sep 2013; published 18 Oct 2013

14. M. Rahm, D. Schurig, D. A. Roberts, S. A. Cummer, D. R. Smith, and J. B. Pendry, "Design of electromagnetic cloaks and concentrators using form-invariant coordinate transformations of Maxwell's equations," Photon. Nanostr. Fundam. Appl. **6**(1), 87–95 (2008).
15. M. Rahm, S. A. Cummer, D. Schurig, J. B. Pendry, and D. R. Smith, "Optical design of reflectionless complex media by finite embedded coordinate transformations," Phys. Rev. Lett. **100**(6), 063903 (2008).
16. T. C. Han, C. W. Qiu, and X. H. Tang, "Adaptive waveguide bends with homogeneous, nonmagnetic, and isotropic materials," Opt. Lett. **36**(2), 181–183 (2011).
17. A. Greenleaf, Y. Kurylev, M. Lassas, and G. Uhlmann, "Electromagnetic wormholes and virtual magnetic monopoles from metamaterials," Phys. Rev. Lett. **99**(18), 183901 (2007).
18. Y. Lai, J. Ng, H. Y. Chen, D. Z. Han, J. Xiao, Z. Q. Zhang, and C. T. Chan, "Illusion Optics: The Optical Transformation of an Object into Another Object," Phys. Rev. Lett. **102**(25), 253902 (2009).
19. W. X. Jiang, C. W. Qiu, T. C. Han, S. Zhang, and T. J. Cui, "Creation of ghost illusions using wave dynamics in metamaterials," Adv. Funct. Mater. **23**(32), 4028–4034 (2013).
20. W. Lu, Z. Lin, H. Y. Chen, and C. T. Chan, "Transformation media based super focusing antenna," J. Phys. D Appl. Phys. **42**(21), 212002 (2009).
21. W. X. Jiang, T. J. Cui, H. F. Ma, and Q. Cheng, "Layered high-gain lens antennas via discrete optical transformation," Appl. Phys. Lett. **93**(22), 221906 (2008).
22. P.-H. Tichit, S. N. Burokur, D. Germain, and A. de Lustrac, "Design and experimental demonstration of high-directive emission with transformation optics," Phys. Rev. B **83**(15), 155108 (2011).
23. Y. Luo, J. Zhang, L. Ran, H. Chen, and J. A. Kong, "Controlling the emission of electromagnetic source" PIER. Online. **4**(7), 795–800 (2008).
24. W. X. Jiang, T. J. Cui, G. X. Yu, X. Q. Lin, Q. Cheng, and J. Y. Chin, "Arbitrarily elliptical-cylindrical invisible cloaking," J. Phys. D **41**(8), 085504 (2008).
25. C. Li and F. Li, "Two-dimensional electromagnetic cloaks with arbitrary geometries," Opt. Express **16**(17), 13414–13420 (2008).
26. H. Ma, S. Qu, Z. Xu, and J. Wang, "The open cloak," Appl. Phys. Lett. **94**(10), 103501 (2009).
27. T. C. Han, C. W. Qiu, and X. H. Tang, "The general two-dimensional open-closed cloak with tunable inherent discontinuity and directional communication," Appl. Phys. Lett. **97**(12), 124104 (2010).
28. D. Schurig, J. J. Mock, B. J. Justice, S. A. Cummer, J. B. Pendry, A. F. Starr, and D. R. Smith, "Metamaterial electromagnetic cloak at microwave frequencies," Science **314**(5801), 977–980 (2006).
29. B. Kante, D. Germain, and A. Lustrac, "A experimental demonstration of a nonmagnetic metamaterial cloak at microwave fequency," Phys. Rev. B **80**(20), 201104 (2009).
30. S. Xu, X. Cheng, S. Xi, R. Zhang, H. O. Moser, Z. Shen, Y. Xu, Z. Huang, X. Zhang, F. Yu, B. Zhang, and H. Chen, "Experimental demonstration of a free-space cylindrical cloak without superluminal propagation," Phys. Rev. Lett. **109**(22), 223903 (2012).
31. J. Li and J. B. Pendry, "Hiding under the carpet: a new strategy for cloaking," Phys. Rev. Lett. **101**(20), 203901 (2008).
32. L. H. Gabrielli, J. Cardenas, C. Poitras, and M. Lipson, "Silicon nanostructure cloak operating at optical frequencies," Nat. Photonics **3**(8), 461–463 (2009).
33. J. Valentine, J. Li, T. Zentgraf, G. Bartal, and X. Zhang, "An optical cloak made of dielectrics," Nat. Mater. **8**(7), 568–571 (2009).
34. F. Zhou, Y. Bao, W. Cao, C. T. Stuart, J. Gu, W. L. Zhang, and C. Sun, "Hiding a realistic object using a broadband terahertz invisibility cloak," Sci Rep **1**, 78 (2011).
35. D. Liang, J. Gu, J. Han, Y. Yang, S. Zhang, and W. L. Zhang, "Robust large dimension terahertz cloaking," Adv. Mater. **24**(7), 916–921 (2012).
36. H. F. Ma and T. J. Cui, "Three-dimensional broadband ground-plane cloak made of metamaterials," Nat Commun **1**(3), 21 (2010).
37. X. Z. Chen, Y. Luo, J. J. Zhang, K. Jiang, J. B. Pendry, and S. Zhang, "Macroscopic invisibility cloaking of visible light," Nat Commun **2**, 176–181 (2011).
38. B. L. Zhang, T. Chan, and B. I. Wu, "Lateral shift makes a ground-plane cloak detectable," Phys. Rev. Lett. **104**(23), 233903 (2010).

1. Introduction

Transformation optics (TO) as a new method to manipulate transmission paths of electromagnetic waves has attracted much attention [1–6]. The fundamental principle of TO is the form-invariant of Maxwell's equations between the physical space and the virtual space [7], by which many fantastic phenomena/devices such as cloaks, field-rotating devices, wave concentrators, beam splitters, waveguide bends, artificial wormholes, illusion systems and antennas are realized [8–23]. Among them, one of the most important and typical applications is the invisible cloak, which makes free space squeezed into a shell, resulting in a hidden region in physical space. J. B. Pendry first proposes this TO-based cylindrical cloak [1], and then many other kinds of cloaks such as square cloaks, elliptical cloaks, arbitrary shaped

#195925 - $15.00 USD Received 20 Aug 2013; revised 20 Sep 2013; accepted 20 Sep 2013; published 18 Oct 2013

cloaks, and open cloaks are reported [13, 24–27]. Since electromagnetic cloaks usually need extremely complex constitutive parameters (inhomogeneous, anisotropic, and especially singular), just simplified strategies (such as reduced cloaks) are adopted to experimental verification of the traditional cloaks [28–30]. However, the reduced cloaks inevitably bring about some side effects in the cloaking efficiency (In other words, it is just an imperfect cloak, and scattered fields appear when electromagnetic waves interacting with the reduced cloak.). To overcome these imperfections, carpet cloaks based on quasi-conformal mapping are proposed and demonstrated experimentally from microwave to optical frequencies [31–37]. However, the quasi-conformal mapping strategy generally results in a lateral shift of the scattered wave, whose value is comparable to the height of the cloaked object, making the object detectable [38]. In addition, this kind of carpet cloak is only able to hide object pressed against the ground plane.

In this paper, composite optical transformation is applied to design singular parameter-independent rotatable illusion media. Electromagnetic waves can be rotated (or bended) and compressed simultaneously, inside the rotatable illusion media. The rotatable illusion media can make the incident light beam bend around the objects without any scattered fields, for the incident light with specific incident directions and certain widths. In other words, when an object is covered with the rotatable illusion media, the incident light beam is bended around the object without interacting with the object, resulting in the singular parameter-independent cloaks. Such a kind of rotatable illusion media can also be used to design tunable miniaturized high-directivity antenna, which can overcome the bottleneck of the device itself which limits the possibility of size reduction. The other characteristic is that the radiation direction of the miniaturized high-directivity antenna can be tunable/rotatable, which may have potential application in wireless communication systems, especially for the indoor wireless secure access.

2. The general modes

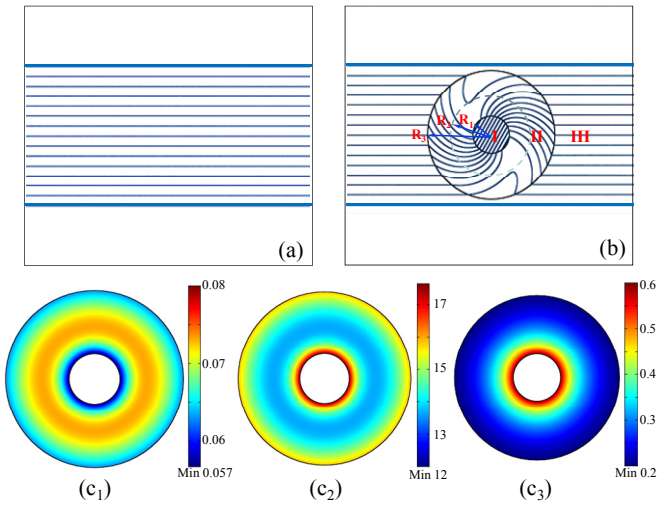

Fig. 1. The principle and parameter distribution of the rotatable illusion media. (a) The power flow in isotropic and homogeneous material (air) illuminated by plane wave. (b) The power flow of the plane wave propagates in a free space (air) embedded with a rotatable illusion media. (c_1-c_3) The parameter distribution of $\mu_1(c_1)$, $\mu_2(c_2)$, $\varepsilon_z(c_3)$ of the rotatable illusion media.

Figures 1(a) and 1(b) illustrate the two-dimensional case of the power flow of plane wave propagating in free space and the rotatable illusion media, respectively. When plane wave interacting with the rotatable illusion media, the power flow streamlines are bended and compressed in region II (transformation region in $R_1<r<R_3$) and region I (compression region

#195925 - $15.00 USD Received 20 Aug 2013; revised 20 Sep 2013; accepted 20 Sep 2013; published 18 Oct 2013

in $r<R_1$), respectively. The corresponding electric permittivity and magnetic permeability tensors of the rotatable illusion media can be calculated as follows:

$$\begin{cases} \overline{\varepsilon}' = \Lambda \overline{\varepsilon} \Lambda^T / \det(\Lambda) \\ \overline{\mu}' = \Lambda \overline{\mu} \Lambda^T / \det(\Lambda) \end{cases}, \tag{1}$$

where $(\overline{\varepsilon}, \overline{\mu})$ and $(\overline{\varepsilon}', \overline{\mu}')$ are the permittivity and permeability tensors in the virtual space and the physical space, respectively. Λ is the Jacobian transformation matrix.

The coordinate transformation between virtual space and physical space in region II can be written as

$$\begin{cases} r' = \dfrac{R_3 - R_1}{R_3 - R_2} r - \dfrac{R_2 - R_1}{R_3 - R_2} R_3 \\ \theta' = \theta + \alpha \dfrac{R_3 - r'}{R_3 - R_1} \\ z' = z \end{cases}, \tag{2}$$

where α is the rotation angle.

The corresponding Jacobian transformation matrix can be expressed as

$$\Lambda = \begin{bmatrix} p & 0 & 0 \\ -\dfrac{\alpha p r'}{R_3 - R_1} & \dfrac{r' p}{r' + q} & 0 \\ 0 & 0 & 1 \end{bmatrix}, \tag{3}$$

in which $p = \dfrac{R_3 - R_1}{R_3 - R_2}$, $q = \dfrac{R_3 (R_2 - R_1)}{R_3 - R_2}$, and $R_1 < R_2 < R_3$.

By using the theory of transformation optics, the permittivity $\overline{\varepsilon}'$ and permeability $\overline{\mu}'$ in region II can be written as follows:

$$\begin{aligned} \overline{\varepsilon}' = \overline{\mu}' &= \begin{bmatrix} \mu_{xx} & \mu_{xy} & 0 \\ \mu_{xy} & \mu_{yy} & 0 \\ 0 & 0 & \varepsilon_{zz} \end{bmatrix} \\ &= \begin{bmatrix} A_{rr} \cos^2\theta - 2A_{r\theta} \sin\theta \cos\theta + A_{\theta\theta} \sin^2\theta & (A_{rr} - A_{\theta\theta}) \sin\theta \cos\theta + A_{r\theta}(\cos^2\theta - \sin^2\theta) & 0 \\ (A_{rr} - A_{\theta\theta}) \sin\theta \cos\theta + A_{r\theta}(\cos^2\theta - \sin^2\theta) & A_{rr} \sin^2\theta + 2A_{r\theta} \sin\theta \cos\theta + A_{\theta\theta} \cos^2\theta & 0 \\ 0 & 0 & \dfrac{r'+q}{r' p^2} \end{bmatrix}, \end{aligned} \tag{4}$$

where $A_{rr} = \dfrac{r'+q}{r'}$, $A_{r\theta} = -\dfrac{\alpha(r'+q)}{R_3 - R_1}$ and $A_{\theta\theta} = \dfrac{(r'+q)^2 r' \alpha^2 + r'(R_3 - R_1)^2}{(r'+q)(R_3 - R_2)^2}$ (Here, $R_1 < r' < R_3$ and $\alpha \supseteq (0, 2\pi)$). All of the values in Eq. (4) are independent of singular parameters. Therefore, the following cloaks based on this illusion media in Eq. (4) are the singular parameter-independent cloaks.

According to Eq. (4), permittivity and permeability tensors have non-diagonal components because of the non-conformal transformations. Based on the rotation transformation, the dielectric tensors in region II can be diagonalized, and the corresponding material parameters in eigen-basis can be expressed as

#195925 - $15.00 USD Received 20 Aug 2013; revised 20 Sep 2013; accepted 20 Sep 2013; published 18 Oct 2013

$$\begin{cases} \mu_1 = \dfrac{\mu_{xx} + \mu_{yy} - \sqrt{(\mu_{xx} - \mu_{yy})^2 + 4\mu_{xy}^2}}{2} \\ \mu_2 = \dfrac{\mu_{xx} + \mu_{yy} + \sqrt{(\mu_{xx} - \mu_{yy})^2 + 4\mu_{xy}^2}}{2} \\ \varepsilon_z = \varepsilon_{zz} \end{cases}, \tag{5}$$

In this case, all the off-diagonal components equal zero, and the components of μ_1, μ_2 and ε_z are finite (non-singularity) and positive for $\alpha = \pi/3$, $R_1 = 0.267$mm, $R_2 = 0.8$mm, $R_3 = 0.933$mm, as shown in Fig. 1(c) (Actually, these components are also finite and positive for $\alpha \supseteq (0, 2\pi)$). All of these components in Eq. (5) are also independent of singular parameters.

The transformation equations in region I can be written as

$$\begin{cases} r' = (R_2 / R_1) r \\ \theta' = \theta \\ z' = z \end{cases}, \tag{6}$$

which means that the region of $r<R_2$ is compressed into region I. The corresponding permittivity $\bar{\varepsilon}'$ and permeability $\bar{\mu}'$ in region I are

$$\bar{\varepsilon}' = \bar{\mu}' = \begin{bmatrix} 1 & 0 & 0 \\ 0 & 1 & 0 \\ 0 & 0 & (R_2 / R_1)^2 \end{bmatrix}. \tag{7}$$

3. Numerical simulations and discussions

First, we investigate the functionalities of the rotatable illusion media shown in Fig. 2. The plane wave propagates from the left side with frequency of 7.5 THz. Figure 2(a) shows the electric field distribution of the plane wave interacting with the illusion media for $\alpha = 0°$. The electric distribution is twisted (bending from its out to core in x-axis) in region II and compressed into region I. In this situation, the illusion media is typically wave concentrator like in Ref [14]. For $\alpha \neq 0°$, the corresponding electric distribution is quite different from the case of $\alpha = 0°$. Figure 2(b) displays the electric distribution of the rotatable illusion with plane wave illuminated from the left side for $\alpha = 90°$. Obviously, the electric field is rotated and twisted in region II. Meanwhile, the plane wave changes its direction for $\pi/2$ inside region I. That is to say, the electromagnetic field distribution can be rotated and compressed simultaneously via the rotatable illusion media.

#195925 - $15.00 USD Received 20 Aug 2013; revised 20 Sep 2013; accepted 20 Sep 2013; published 18 Oct 2013

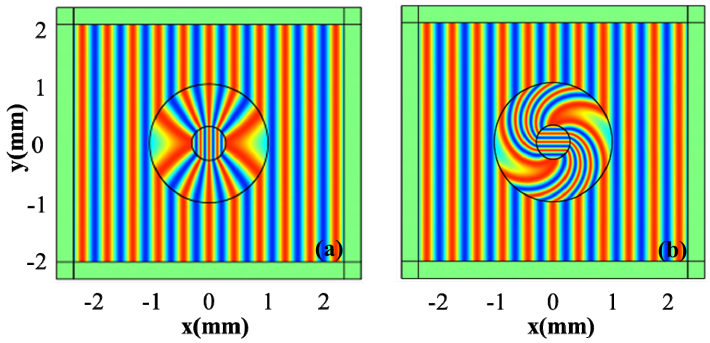

Fig. 2. Electric field distribution of the rotatable illusion, when the plane wave propagating from the left side with $\alpha = 0°$(a) and $\alpha = 90°$.

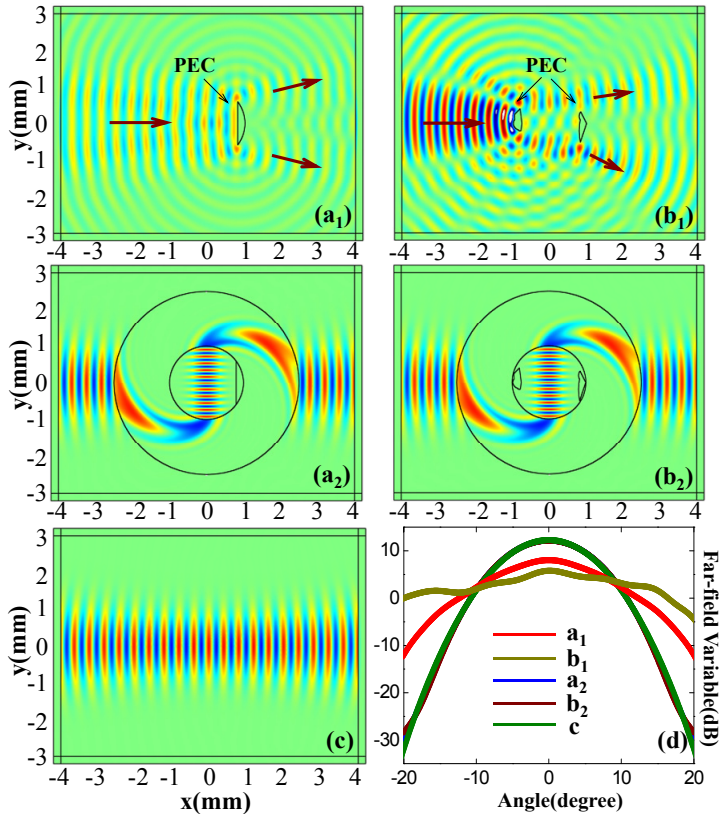

Fig. 3. Electric field distribution when a Gaussian beam is launched from the left side and scattered with a semi-ellipse shaped PEC (a_1) or two arbitrary-shaped PECs (b_1). (a_2) and (b_2) are the same as (a_1) and (b_1), but both of them are covered with the rotatable illusion for $\alpha = 90°$. (c) Electric field distribution in free space when a Gaussian beam is launched from the left side. (d) The corresponding far-field patterns of (a_1) (red curve), (b_1) (dark yellow curve), (a_2) (blue curve), (b_2) (wine curve), (c) (green curve).

Now, we study the singular parameter-independent cloaks by using the rotatable illusion media. As discussed in Eqs. (5) and (7), the corresponding permittivity and permeability of the rotatable illusion media are finite (non-singularity) and positive. When the incident Gaussian beam with a certain width propagates from specific incident directions, a singular

#195925 - $15.00 USD Received 20 Aug 2013; revised 20 Sep 2013; accepted 20 Sep 2013; published 18 Oct 2013

parameter-independent cloak can be realized by using this rotatable illusion media, as shown in Fig. 3. Here, it is important to note that the incident Gaussian beam should be limited in a small width. According to the coordinate transformation, the electromagnetic field in region of $r<R_2$ can be rotated and compressed into region I ($r<R1$) completely, so the width of the Gaussian beam in this paper must be less than R_2. Figures 3(a_1) and (b_1) depict the electric field distributions of a Gaussian beam with a frequency of 7.5 THz propagating from the left side. When the Gaussian beam interacts with a bare semi-ellipse

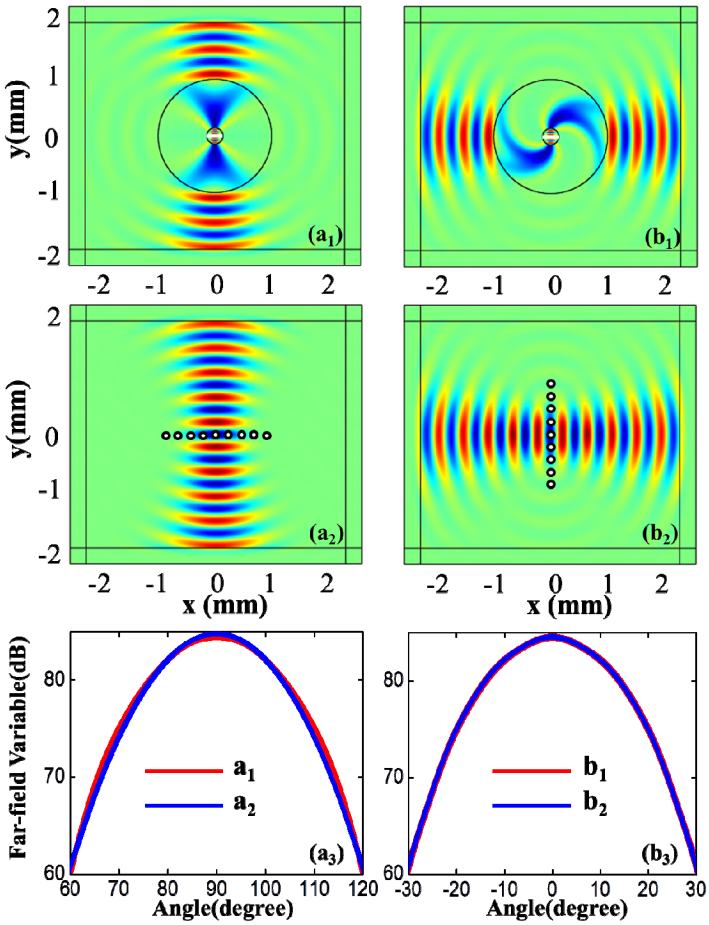

Fig. 4. Electric field distributions of tunable miniaturized high-directivity antenna. (a_1) and(b_1) are the electric field distributions of two identical small antenna arrays embedded in the rotatable media with $\alpha = 0°, 90°$, respectively. (a_2) and(b_2) are the two corresponding electric field distributions of two larger antenna arrays. (a_3) is the far-field patterns of (a_1) and(a_2), while (b_3) is the far-field patterns of (b_1) and(b_2).

shaped PEC (perfect electrical conductivity) or two bare arbitrary-shaped PECs, strong scattered fields appear in the electric field distributions, as shown in Figs. 3(a_1) and (b_1). The corresponding far-field patterns are shown in Fig. 3(d) by the red and dark yellow curves, respectively. However, when both of the semi-ellipse shaped PEC and the two arbitrary-shaped PECs are covered by the rotatable illusion media with incident angle of $\alpha = 90°$, as shown in Figs. 3(a_2) and 3(b_2), respectively, the incoming Gaussian beam is bended around these PECs and does not interact with them. In other words, when the Gaussian beam shines on these PECs, the rotatable illusion media guides the Gaussian beam rotating with angle of

#195925 - $15.00 USD Received 20 Aug 2013; revised 20 Sep 2013; accepted 20 Sep 2013; published 18 Oct 2013

90°, and avoid the Gaussian beam interacting with these PECs. Figure 3(c) depicts the electric field distribution of the same Gaussian beam propagating in free space. Comparing with Figs. 3(a_2), 3(b_2), and 3(c) and the far-field patterns in Fig. 3(d), the PECs in Figs. 3(a_2) and 3(b_2) are invisible. We want to emphasize that such a kind of invisible cloak is singular parameter-independent (shown in Eqs. (5) and (7) compared with the traditional cylindrical-shaped cloak (The fundamental mechanism of traditional cloak is that a point in free space is expanded as a finite space, leading to the singular parameters-dependent transformation media.). As discussed above, the basic principle of our cloak is quite different from the case of the traditional cylindrical-shaped cloak.

Finally, we discuss a potential application of tunable miniaturized high-directivity antennas via this kind of rotatable illusion media. Although miniaturization and integration are inevitable trends in the development of telecommunication devices such as the tunable miniaturized high-directivity antenna, in many cases, it is the device itself that limits the possibility of size reduction and tunability. Here, our rotatable illusion media maybe a possible way to solve these bottleneck problems, because this media has the rotation and compression functions, simultaneously. Figures 4(a_1) and 4(b_1) show the electric field distributions of two small identical antenna arrays located in the central region of the rotatable illusion media for $\alpha = 0°$ and $\alpha = 90°$, respectively. Here, we take a nine-element antenna array design as an example, and the current distribution on each element is set to be 1/70:4/35:2/5:4/5:1:4/5:2/5:4/35:1/70. In this case, the length of the antenna arrays is 0.0267*mm*. Compared with Fig. 4(a_1), the radiation field in Fig. 4(b_1) rotates anticlockwise with angle of 90°, although both of these two small antenna arrays are organized along x-axis. Figures 4 (a_2) and 4(b_2) display the radiation field distributions of two large antenna arrays (But, the length of the antenna arrays is 0.16 *mm*). Both of these two large antenna arrays are identical with each other, but they are organized along x-axis and y-axis, respectively. Therefore, the radiation field in Figs. 4(a_2) and 4(b_2) are orthogonal to each other. The corresponding far-field patterns are shown in Figs. 4(a_3) and 4(b_3). Comparing with Figs. 4(a_1) (Figs. 4(b_1)), 4(a_2) 4(b_2) and 4(a_3) (4 (b_3)), a large antenna array can be replaced by a small one covered with the illusion media. In addition, the direction of the radiation field can be well controlled by this illusion media. In a word, a tunable and miniaturized high-directivity antenna is realized by using our rotatable illusion media (with positive permittivity and permeability).

4. Conclusion

In conclusion, a rotatable illusion media with finite (non-singularity) and positive permittivity and permeability have been proposed and investigated. The incident Gaussian beam can be bended inside the rotatable illusion media. So, objects covered with the rotatable illusion media can be hidden by guiding the incident beam (with certain width and specific incident direction) bending around them, leading to singular parameters-independent cloaks. Such a kind of rotatable illusion media can also be applied to design tunable miniaturized high-directivity antenna, which may have potential application in future indoor wireless secure access system.

Acknowledgments

This work is partly supported by the Major National Development Project of Scientific Instrument and Equipment (2011YQ150021) (2012YQ150092), the Key Scientific and Technological Project of Science and Technology Commission of Shanghai Municipality (12142200100) (12JC1407100), National Natural Science Foundation of China (61307126) (11174207) (61138001) (61007059) (61205094), the Leading Academic Discipline Project of Shanghai Municipal Government (S30502), and the Scientific Research Innovation Project of Shanghai Municipal Education Commission (14YZ093).